Journal of Materials Chemistry A

Accepted Manuscript

ROYAL SOCIETY OF CHEMISTRY

www.rsc.org/materialsA

Journal of Materials Chemistry A

ARTICLE

Metal chalcogenides as counter electrode material in quantum dot sensitized solar cells: a perspective

Received 00th January 20xx,
Accepted 00th January 20xx

DOI: 10.1039/x0xx00000x

www.rsc.org/

Ke Meng [a], Gang Chen[a*] and K. Ravindranathan Thampi[b*]

Quantum dot sensitized solar cell (QDSSC), which has analogue structure and working principle with dye sensitized solar cell, has drawn much attention due to its characteristic advantages like ease of fabrication, robustness and the potential for multiple electron generation. Numerous efforts to optimize various components of QDSSCs have been taken to boost the overall device performance. It is well known that counter electrode (CE) plays a vital role in sensitized solar cells and could profoundly impact the device performance. Recently, metal chalcogenides have been explored as superb counter electrode material for QDSSCs. This review gives a panorama of both conventional noble metal and carbon CE and newly emerged metal chalcogenide CE materials for QDSSCs, while the influence of CE materials on the overall device performance is stressed in detail. Conclusion and prospect emphasizes the importance of the studies on metal chalcogenide CE materials and put forward remaining challenges to be addressed.

1. Introduction

Renewable energy sources are increasingly preferred over fossil fuels for attaining sustainability in our consumption patterns.[1] Among renewables, solar energy is the most abundant energy source, which provides our planet about 10000 times more energy than today's global energy consumption per day.[2] Solar energy can be collected and converted into heat or electricity. Photovoltaic (PV) cells provide a direct way to convert solar energy into electricity with attractive conversion efficiencies.[3-6] The third generation PV comprising of advanced thin films and newer PV concepts promise potentially higher energy conversion efficiencies at lower costs, among which Dye sensitized solar cells[7-10] (DSSC) and Quantum dot sensitized solar cells[11-14] (QDSSC) are particularly promising due to a variety of reasons. DSSCs were first introduced as a third generation solar cell concept in the late 1980s and early 90s.[7] By the application of natural or synthetic organic dyes as sensitizers and mesoporous layers of semiconductors, such as TiO_2, as charge collector and carrier, DSSCs have reached conversion efficiencies of 13%.[15] QDSSCs, similar in principle but replacing dyes by quantum dots (QDs) as light harvesting sensitizers, are considered superior because of the interesting optoelectronic properties of QDs.[14] A quantum dot (QD) is a nanometre-scale semiconductor crystallite.[16] It confines the electron-hole pair in all three dimensions.[16-18] The size attributes a quantum confinement to the particles giving rise to tuneable band gaps, high molar extinction coefficients and large intrinsic dipole moments.[17] Taking advantages of these properties, QDSSCs have reached an efficiency of more than 8%[19], despite its relatively shorter history and much lesser industrial investment.

Over the years, numerous efforts have been taken to improve the overall performance of QDSSCs.[20-29] Different quantum dot synthesis and sensitization methods[30-40], including chemical bath deposition (CBD), successive ionic absorption and reaction (SILAR), direct absorption (DA), linker assisted absorption, electro deposition and atom layer deposition (ALD) etc., were developed, aiming to obtain QDs with superior opto- and electro- chemical properties. While various choices of wide band gap structures (WBGS) for QDSSC, such as materials[41-49] including TiO_2, ZnO, SnO_2, $BaTiO_3$, Nb_3O_7, Nb_3O_7F or Zn_2SnO_4 and structures[50-59] including mesoporous semiconductor film, nanowires, nanorods or nanosheets, were investigated to get enhanced charge transfer and transportation abilities. Researchers have also focused on the development of compatible electrolytes and counter electrodes to attain higher conversion efficiencies and cell stability. The classic I^-/I_3^- electrolytes are not suitable for QDSSC mainly because of the photo-corrosion problem.[60] A variety of alternative electrolytes were investigated[61-67], among which, an aqueous polysulfide electrolyte had proved itself as the most competitive. Counter electrode, where electrons flow back into the electrolyte from external circuit, requires materials with favorable catalytic property and charge transfer ability to better functionalize QDSSCs.[68] This drives the intensive investigation on appropriate counter electrode materials; noble metals, carbon materials, metal sulfides, metal selenides and other alternative counter electrode materials have been successfully introduced in QDSSCs. Among

[a] School of Physical Science and Technology, Shanghaitech University, Shanghai, China.
[b] School of Chemical and Bioprocess Engineering, University College Dublin, Belfield, Dublin 4, Ireland and UCD Earth Institute , University College Dublin, Belfield, Dublin 4, Ireland.

these, metal chalcogenides (metal sulfides and selenides) present the most promising performance. This review gives a thorough overview of this class of promising counter electrode materials and their influence on QDSSC performance.

2. Working Principles of QDSSC

QDSSC has a much similar structure to that of DSSC, where the sensitizer is a QD, instead of a dye.[11-14] Specifically, it comprises a working electrode (WE) and a counter electrode (CE) sandwiched together with an electrolyte or a hole-transporting mediator, as shown in Fig. 1. The WE consists of a transparent fluorine-doped tin oxide (FTO) conducting substrate, a layer of wide band gap semiconductor material film (usually a layer of mesoporous TiO_2) sensitized by QD sensitizers. The counter electrode is built on an FTO conducting substrate with a layer of a catalytic material. With a similar structure, the working mechanism of QDSSC is analogic to that of DSSC, as shown in Fig. 2. The electrons are passed through an external circuit from the WE to the CE. The electrolyte, most commonly a solution of redox couples or a hole-conductor, works as the charge carrier mediator. The working principles of DSSC could also be found in the many review articles on various processes central to the development of QDSSCs published in recent years[69-75].

3. Electrolytes for QDSSCs

The most common electrolyte used in DSSC is I^-/I_3^- electrolyte prepared by mixing I^- and I_2 with other additives in suitable organic solvents.[7, 10, 76] However, experimental results showed that I^-/I_3^- electrolytes are not suitable for QDSSC mainly because of the photo-corrosion problem observed on QDs when applying this electrolyte.[60, 77] Though a study was conducted to protect the QDs from bleaching by coating them with protective layers[78], the overall PCE of the cell remains quite low indicating that suitable alternative electrolytes should be found and used to improve QDSSC performance and its long-term stability.

The photo-degradation of light absorbing semiconductors when in contact with I^-/I_3^- electrolyte has been observed in photo-electrochemical cells (PEC) early in the 1970s.[79, 80] This undesired effect was explained by the fact that the reaction (when CdS is used as light absorbing semiconductor, for example)

$$CdS + 2h^+ \rightarrow Cd^{2+} + S \quad (1)$$

competes with the desired hole injection reaction

$$3I^- + 2h^+ \xrightarrow[CdS]{} I_3^- \quad (2)$$

leading to rapid surface degradation. Such corrosion problems are inherent in most semiconductors with the exception of some wide band gap semiconductors like TiO_2.[81] A S^{2-}/S_n^{2-} redox electrolyte was introduced to lower the anodic potential aiding in solving the stability problem; though at the expense of lowering the driving potential and thus the conversion efficiency.[82-84] Experiment results showed that the S^{2-}/S_n^{2-} redox electrolyte indeed stabilized the photo-electrode and promising power conversion efficiencies were obtained for the PEC devices.

This S^{2-}/S_n^{2-} redox electrolyte was adopted in QDSSC and identified as an efficient and compatible electrolyte.[60, 85] The working mechanism of this redox couple in QDSSC can be explained by the following processes.

The oxidizers in the redox couple collect holes at the photo-electrode (TiO_2/QDs) and more precisely at the electrode-electrolyte interface.

$$S^{2-} + 2h^+ \rightarrow S \quad (3)$$

$$S + S_{n-1}^{2-} \rightarrow S_n^{2-} \ (n = 2-5) \quad (4)$$

After the ion diffusion process in the electrolyte, the oxidized species (the S_n^{2-} ions) are converted back to S^{2-} by collecting electrons at the electrolyte/counter electrode interface.

$$S_n^{2-} + 2e^- \rightarrow S_{n-1}^{2-} + S^{2-} \quad (5)$$

The S^{2-}/S_n^{2-} redox couple is able to mediate the carrier for Cd chalcogenide QDSSCs efficiently. Most of the high efficiency QDSSC reported applied the polysulfide electrolyte.[19, 30, 31, 86] However, it was evidenced that the polysulfide electrolyte was not suitable for PbS QDs because of the photo-corrosion problem, again.[87] By doping the PbS QDs with Hg^{2+} [87] or protecting the PbS QDs with a CdS coating layer[88], considerably high efficiency PbS sensitized solar cells applying the polysulfide electrolyte were also fabricated.

Based on the S^{2-}/S_n^{2-} redox couple, effective efforts have also

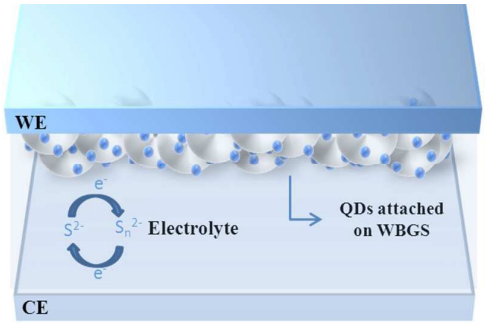

Fig.1 Structure of a typical QDSSC

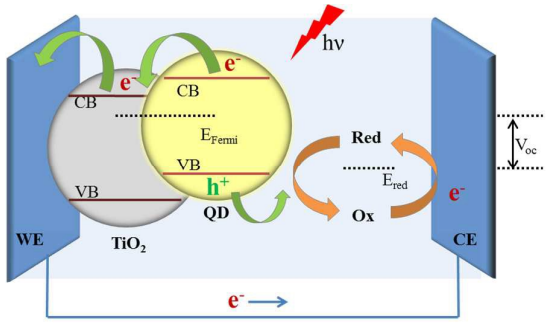

Fig. 2 Scheme of working mechanism of QDSSC

been considered to enhance the polysulfide electrolyte's performance, such as the inclusion of additives or structural modification of the redox couple.[60, 67, 89, 90] KCl[60] and GuSCN[89] have been proved to be effective additives for the electrolyte to help the solar cell's J_{sc}. An organic cation was introduced in the redox couple to replace the commonly counterion Na^+, which significantly improved the FF of solar cells.[67] A sulfide/polysulfide based ionic liquid electrolyte was once prepared for QDSSC as well.[90]

Several solid state electrolytes were applied in QDSSCs to realize solid state devices, which avoids the engineering and vapour toxicity problems arising from leakages and seal degradation due to volatility of low-boiling solvents.[35, 37, 64, 91-93] Hole transporting materials like Spiro-MeOTAD[35, 37], P3HT[91] and CuSCN[94], solid-state ionic conductors involving polysulfide redox species[64, 93] are usually coupled with noble metal CE to functionalize QDSSCs. However, the efficiency of the solid state devices remains lower than the liquid-junction cells. Future studies are expected to investigate in this interesting and exciting field.

Other electrolyte systems, such as Co^{2+}/Co^{3+}, Mn complexes, thiolate/disulfide, Fe^{3+}/Fe^{2+} and $Fe(CN)_6^{3+}/Fe(CN)_6^{4+}$ [61-67] electrolytes have also been tested in QDSSCs. However, results indicate that unless there is a major breakthrough in developing an efficient electrolyte system, researchers have to rely on the polysulfide electrolytes to move the field of QDSSC forward.[12]

4. Counter electrode in QDSSC

Counter electrode (CE) is where electrons flow back into the electrolyte from external circuit. It is evidenced that CE has a vital influence on the solar cell's overall performance.[95] The impact of counter electrode on the performance of QDSSC is mainly derived from the material's conductivity since it provides electron pathways to complete the circuit as well as the catalytic ability to regenerate the reduced species (S^{2-}) in the electrolyte.[96, 97]

The conductivity of the CE is affected by sheet resistance of the FTO substrate, resistance of the counter electrode material and the corresponding contact resistance.[96] It is part of solar cell's series resistance (R_s) which determines one of the solar cell' most important parameter, fill factor (FF). A superiorly conductive CE reduces R_s, thereby improving FF, resulting in a higher efficient QDSSC device.[97]

The catalytic ability of the CE can be rationalized using the term of current density (J), which can be calculated from the charge transfer resistance (R_{ct}), using Equation[21]

$$R_{ct} = RT/nFJ \quad (6)$$

where R is the gas constant, T is the absolute temperature, n is the number of electrons transferred in the elementary electrode reaction and F is the Faraday's constant. The reactions at the CE vary depending on the choice of redox species applied as the charge mediator. When the S^{2-}/Sn^{2-} redox couple is used in QDSSC, the reaction shown in (5) occurs. A more detailed information on the analytic methods for CEs could be found in another quite recent review[98] on QDSSC CE, which also provides great insights into common CE material used in this field.

Efficient CE for QDSSC requires favorable charge transfer ability and catalytic property. To achieve this, a vast of CEs have been studied based on the combination of different materials and structures. In the following sections, CE materials including both the conventional (noble metal and carbon) and the newly emerged metal chalcogenides (copper sulfides, other metal sulfides and metal selenides) will be introduced separately.

5. Noble metal and carbon

5.1 Pt as counter electrode

Pt is a highly catalytic, precious, lustrous, grey-white metal. Its remarkable stability and favorable thermal/electrical properties make it attractive in various applications.[99] Pt is the most common CE material for DSSC, since it possesses appreciable electrocatalytic ability towards I_3^- reduction and superior conductivity.[7-10] In the early stage of the QDSSCs research, the DSSC benchmark Pt material was introduced to catalyze the S^{2-}/S_n^{2-} redox couple.[60, 77, 100] However, these devices exhibited unfavorable power conversion efficiencies, mainly limited by the poor fill factor and short circuit current density. The incompatibility between the polysulfide electrolyte and the Pt counter electrode was pointed out, which was explained by the fact that sulfur-containing compounds adsorb preferably and strongly to the Pt surface thus deduce its catalytic ability and conductivity.[100, 101]

5.2 Au-based materials

In order to better functionalize the polysulfide electrolyte, Au has been studied as an alternative CE material for QDSSCs. Several studies evaluated the influence of replacing Pt with Au as CE material on QDSSC performance.[95, 100, 102] Results have been unanimous that higher PCEs were obtained for Au-containing QDSSC devices indicating Au worked as a better catalytic material. Lee *et al.* designed an experiment to explain this phenomenon where Pt and Au electrodes were introduced to study the adsorption behaviour of S^{2-} on the electrodes and its effect on the surface activity, in the assist of cyclic voltammetry measurement.[100] It was certified that though S^{2-} ions adsorbed on both Pt and Au surfaces, the ions adsorbed more weakly on the Au material (Fig. 3 presents the cyclic voltammograms). Au material in nanoparticle (NP) form has also been applied as CE in QDSSCs for its characteristic properties including high surface area, transmittance and electrical conductivity. Kiyonaga *et al.* examined the catalytic property of Au NPs (Fig. 4a) to reduce S_n^{2-} ions in a photo-electrochemical solar cell using quantum dot-sensitized TiO_2 photoelectrodes[103]; they revealed that the size and crystal orientation control of Au nanoparticles greatly affect their catalytic property. Zhu *et al.* further embedded Au NPs in a graphene network structure to build a reduced graphene

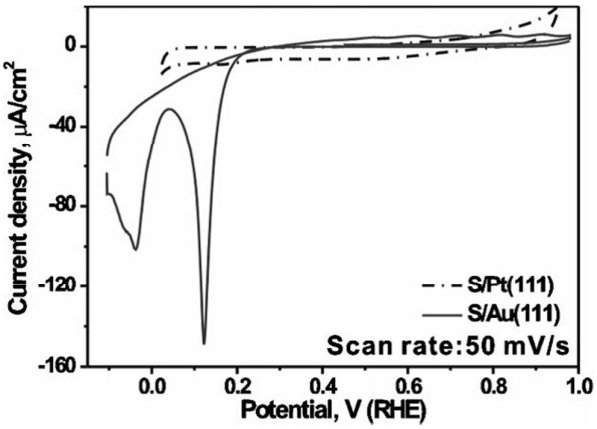

Fig. 3 Cyclic voltammograms for S-modified Au(111) and Pt(111)electrodes recorded at 50mV s^{-1} in 0.1 M $HClO_4$ solution[100]

(RG)–Au NP composite film as CE for QDSSC (Fig. 4b), aiming at combining the high catalytic property of Au NPs and the conductivity of the graphene.[104] From a recent study, it was evidenced that an Au/Pt composite also had enhanced electrocatalytic activity compared to sole Au or Pt material. Yoon *et al.* coated Au on Pt NPs by electro-deposition to form a composite material (Fig. 4 c and d); QDSSCs applying this material as CE showed maximized PCE.[105]

5.3 Carbon

To make efficient and low-cost QDSSCs, alternative CE materials with lower prices and higher catalytic abilities other than noble metal materials should be investigated. Carbon material, a class of material featured as cost-effective, environmental-friendly, earth-abundant, corrosion-resistive and highly catalytic, is quite promising in these regards.[99, 106-108] Various carbon materials, such as carbon black, mesoporous carbon, carbon nanotubes (CNTs), graphene and fullerenes, have been successfully employed as CE materials in the realm of DSSC research.[107, 109-113] The superior conductivity and favorable catalytic ability towards I^-/I_3^- redox couple, plus the low cost of these carbon materials make this class of material a competitive rival. Carbon materials also show catalytic ability towards S^{2-}/S_n^{2-} redox couple.[114, 115] This drives intensive studies on the employment of carbon materials as CEs in QDSSCs.

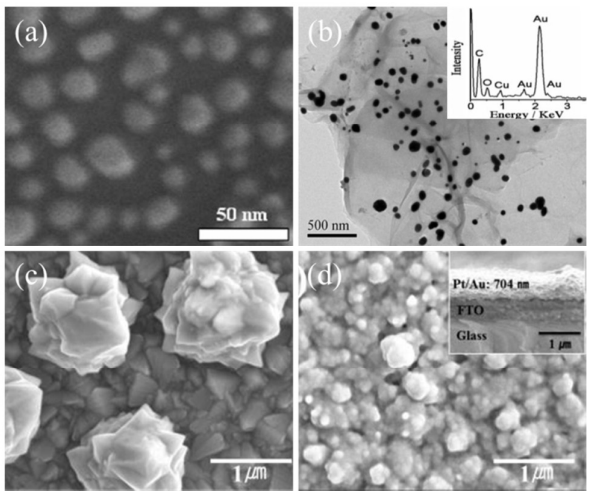

Figure 4: SEM images of (a) Au NPs[103] (b) Au NPs embedded in RG network, inset corresponds to the EDS spectrum[104] (c) Au clusters[105] and (d) Pt coated Au, inset shows cross-sectional SEM images[105]

Fan *et al.* firstly tested activated carbon and hierarchical nanostructured spherical carbon with hollow core/mesoporous shell (HCMS) as CE material in QDSSCs.[116] Solar cell devices consisting either of the two carbon based CEs outperformed devices that employing Pt CE, indicating the better catalytic ability of carbon material over Pt. Results also showed that the HCMS material better functionalize polysulfide electrolyte compared to active carbon. Considering the similar roughness of the two structures, it was argued that the unique structure of HCMS enhanced mass transportation thus led to more efficient diffusion of the reactants and products in the electrolyte's redox reactions. A PCE of 3.9% was obtained for solar cells applying HCMS CE while the R_{ct} between this CE and polysulfide electrolyte was measured as 12 Ω cm^2. The authors further developed an ordered multimodal porous carbon (OMPC) CE structure.[117] QDSSCs using this CE exhibited even better PCE of 4.36% and R_{ct} of 3.5Ω cm^2, mainly due to the improvement in mass transportation resulted from the interconnected multimodal pore framework. Other carbon materials, including ordered mesocellular carbon foam[118, 119], hollow core-mesoporous shell carbon[120], nitrogen-doped hollow carbon nanoparticles[121] and vertically aligned single-walled carbon nanotubes[122], were also designed and prepared as efficient CE materials for QDSSCs.

Despite intensive research, the PCE of QDSSCs employing carbon based CEs remain lower than 5% for the best. The lowest R_{ct} reported between carbon CE and polysulfide electrolyte is 3.5Ω cm^2, which is still one order of magnitude higher than that of Pt towards triiodides in DSSCs.[117, 123] These values suggest that carbon CE might not be a perfect choice for polysulfide reduction; however, its superior conductivity makes it a proper conductive substrate to prepare hybrid material as efficient CE for QDSSCs. It remains to be seen whether judicious alteration of material architectures, especially at the interfacial levels, influence favourably the R_{ct} and bring it down to values comparable to that of I^-/I_3^- measured with Pt. The wide spread interest in carbon materials, especially graphene based, is expected to dwell on such possibilities in the near future.

6. Metal chalcogenides as CE in QDSSC

6.1 Copper sulfides materials

Since the discovery of CdS/Cu_2S heterojunction solar cells in 1954[124], copper sulfides have drawn much attention as a highly useful component in photovoltaic cells. A suitable band gap of 1.1–1.4 eV and a high absorption coefficient of 10^4 cm^{-1} render copper sulfides a possibly ideal class of material with low cost and low toxicity.[125] It is well known that copper sulfides can be obtained with different phases, from the Cu_2S in the 'sulfur

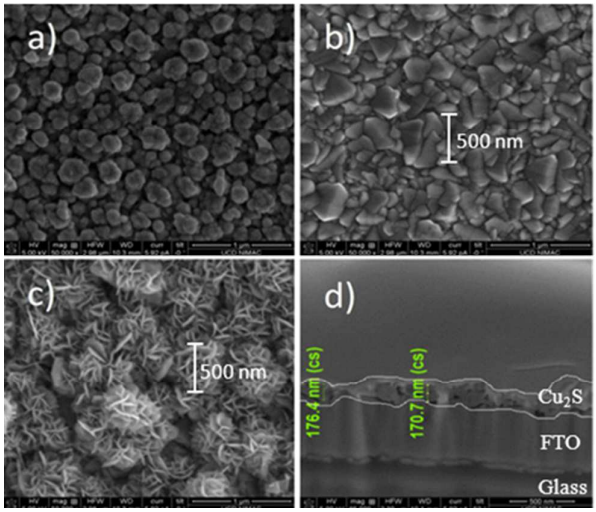

Fig. 5 (a) SEM images of bare FTO glass (b) SEM images of Cu plated FTO glass (c) SEM images of Cu_2S coated FTO glass and (d) Cross section SEM image of Cu_2S coated FTO glass (Cu_2S layer highlighted manually)[51]

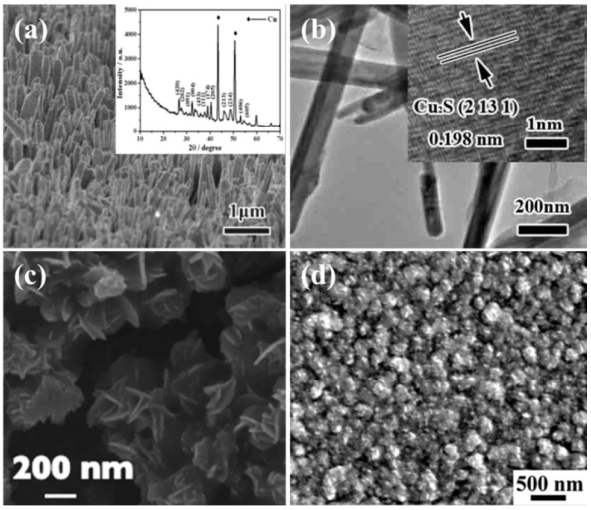

Fig.7 SEM and TEM images of Cu_2S nanostructures prepared using (a) and (b) CBD (nanorod)[127] (c) spray deposition[128] and (d) vapor deposition method[129], inset of a is the XRD pattern of the Cu_2S nanorod

rich region' to CuS in the 'copper rich region'. The complex structures and valence states of Cu_xS endow themselves with interesting physical and electrochemical properties. Studies have shown that Cu_xS possesses superior catalytic ability towards the reduction of S_n^{2-}.[84, 95, 115] This makes it promising as efficient CE material in QDSSCs.

6.1.1 Cu_2S

Cu_2S is a p-type semiconductor with reported bandgap of 1.1–1.4 eV and has a wide application in solar cells.[126] In the 1980s, Hodes *et al.* found that Cu_2S-based CE possesses superior advantages when working with polysulfide electrolytes in a photo-electrochemical cell (PEC).[115] The Cu_2S CE was fabricated by exposing etched brass gauze in a polysulfide solution. This CE was adopted in QDSSC, which resulted in an enhancement of device performance.[43, 95] Specifically, the FF and J_{sc} were dramatically enhanced due to the CE's improved catalytic property. Despite the outperformance of the Cu_2S material, Cu_2S CE prepared in this manner suffers from stability problems over a long period of time, which is mainly due to the fact that the residual Cu in the brass substrate constantly reacts with the electrolyte leading to ultimate disintegration of the CE film itself.[101, 115, 130] Also, the poor mechanical stability and relatively low surface area of the Cu_2S film also affect its performance as CE. In these regards, novel Cu_2S CE preparation methods were developed, aiming at obtaining CEs with better stability, conductivity and catalytic ability.

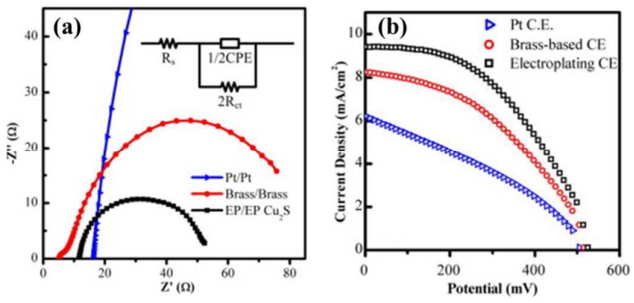

Fig. 6 (a) Nyquist plots of symmetric cells based on different counter electrodes, inset is the equivalent circuit to simulate the EIS curves and (b) J-V curves of cells applying different kinds of counter electrodes[51]

To avoid the aforementioned problems, FTO conducting glasses are introduced to replace brass as substrate to deposit Cu_2S film. The electroplating approach was firstly introduced by our group to deposit porous Cu_2S films on FTO substrates.[51] The CE was fabricated using a two-step method by first electrodepositing a thin layer of Cu on FTO, followed by a polysulfide treatment. The preparation process is depicted by SEM images shown in Fig. 5. The final Cu_2S film composing of 20-50 nm thick nanosheets possesses a porous, flower-like structure and has a thickness between 100 and 200 nm. The favorable structure gives the film superior catalytic ability. The charge transfer resistance between the Cu_2S film and the polysulfide electrolyte was calculated to be a relatively low value of 5.7 Ω/cm^2, while a promising PCE of 2.6% was obtained for CdS QDSSC applying this novel CE (Fig. 6). Cu_2S CE prepared using a similar method was introduced in CdSSe and CdSeTe QDSSCs, resulting in the PCEs as high as 5.41%[131] and 6.36%[30], respectively. Other methods, including chemical bath deposition[127, 132, 133], spray deposition[128, 134], screen-printing[135] and vapor deposition[129] were also introduced to deposit Cu_2S films on FTO substrate, leading to various film morphologies and properties (Fig. 7). These efforts significantly improved the catalytic property and stability of CEs.

The catalytic property and electrical conductivity are two main factors determining the performance of a CE.[136] Cu_2S films coated on FTO substrates provide CEs with good catalytic ability but undesirable electrical conductivity due to the intrinsically poor conductivity of Cu_2S. Thus, composite materials made by hybridizing Cu_2S with conductive species are deposited on FTO substrate to form CE structures with both superior catalytic activity and conductivity. Among these

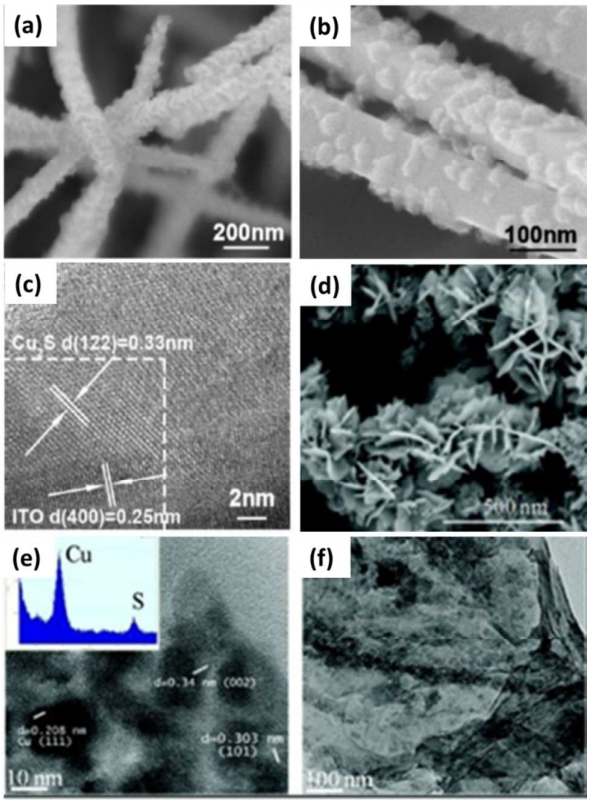

Fig. 8 (a) Low-magnification (b) high-magnification SEM images of ITO@Cu_2S (c) HRTEM image showing the interface of Cu_2S nanocrystal shell and ITO nanowire core[137] (d) SEM image of the RGO-Cu_2S composite (e) TEM image of the Cu_2S nanoparticles embedded into the RGO matrix along with some residual Cu^0 and (f) TEM image defocused to show the RGO sheet within the composite[101] Adapted with permission from ref. 101, 137 Copyright 2013 American Chemical Society

CE structures, a rationally designed core-shell structure developed by Jiang *et al.* was particularly interesting and performed promisingly.[137] In this structure, a tin-doped indium oxide nanowire (ITO) core works as a three-dimensional conductive network and a degenerate p-type Cu_2S nanocrystal shell functionalized as catalyst (Fig. 8 a-c presents the SEM and TEM images of the composite material). Also, this core-shell structure configured tunnel junction arrays which could facilitate charge transfer and transportation processes. Thus, the new design significantly decreased the charge transfer resistance and sheet resistance of the CE, resulting in a 35% enhancement in QDSSC PCE compared to its Cu_2S-film rival. This CE structure was further optimized by engineering the ITO/Cu_2S interfaces achieved by varying synthetic methods.[138] Kamat' group developed another highly efficient CE structure by composing Cu_2S nanocrystals into reduced graphene oxide (RGO) (Microscopic pictures shown in Fig. 8 d-f).[101] Taking advantages of RGO's ability to stabilize metal nanoparticles, Cu particles were firstly spread onto the RGO mat and then converted into Cu_2S by immersing in polysulfide solution. The CE was finally obtained using an *ex-situ* method by doctor-blading the resulted Cu_2S/RGO composite on a FTO substrate. The high surface area of the 2D RGO mat promotes high numbers of Cu_2S reactive sites, while the conductivity of the

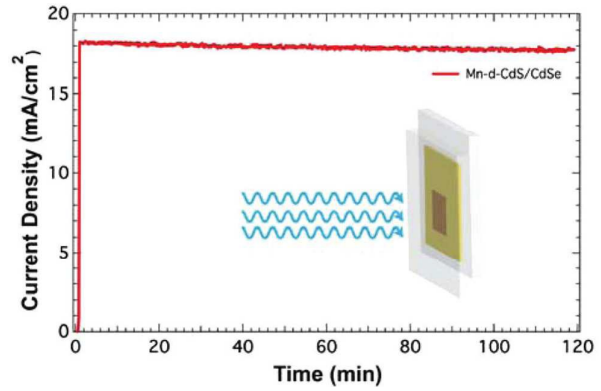

Fig. 9 Photocurrent stability of Mn-doped-CdS/CdSe QDSSC under continuous illumination (100 mW/cm^2) Inset shows the schematic design of the sandwich-solar cell (Cu_2S/RGO counter electrode and aqueous 1 M S^{2-}/1 M S as electrolyte)[41] Reprint with permission from ref. 41 Copyright 2012 American Chemical Society

composite material enables efficient electron shuttling. These positive factors guaranteed the outperformance of this CE over Pt electrode, indicated by a dramatic improvement of ~75% in QDSSC fill factor. The same CE also showed encouraging performance and stability when incorporated in a Mn-doped CdS/CdSe QDSSC; a PCE of 5.4% was obtained while a steady photocurrent was delivered over 2 h of illumination, as shown in Figure 9.[41] Following this, a one-step method was developed by Ye et al. to prepare a similar Cu_2S/RGO composite, resulting in enhanced performance.[139] There are also a few studies compositing Cu_2S with carbon black to fabricate QDSSC CE.[140, 141] Though the lab-size QDSSCs

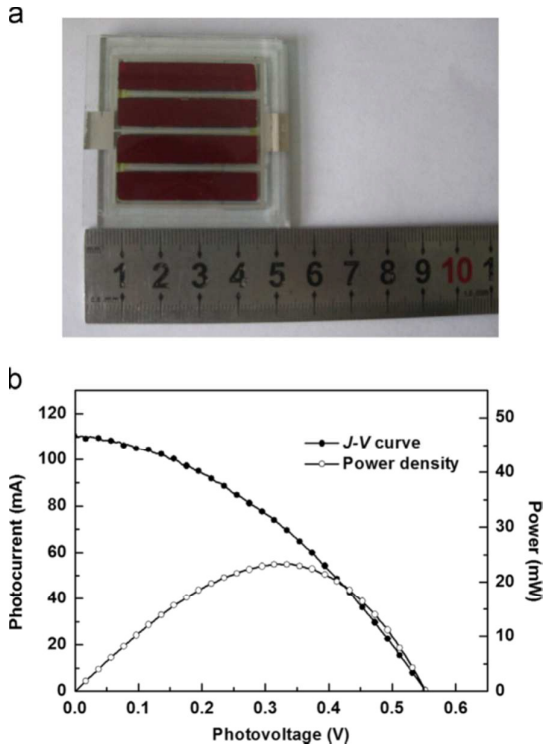

Fig. 10 (a) Digital photo and (b) J–V curve and power density (under AM1.5 illumination) of the 12.97 cm^2 CdS/CdSe QDSSC module[141]

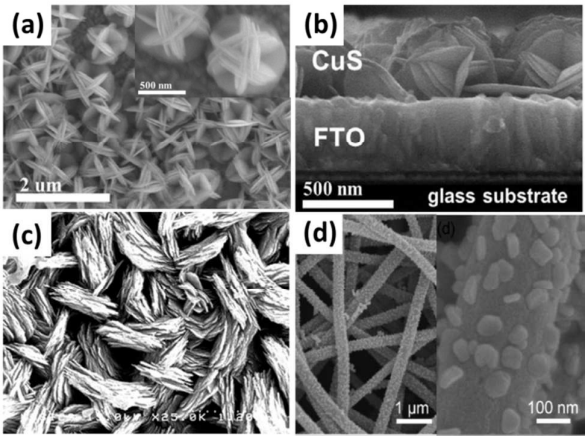

Fig. 11 SEM images of (a) hierarchical CuS prepared by electrodeposition[142] (b) electrodeposited CuS CE's cross section[142] (c) knit coir mat structured CuS film[143] and (d) CuS/electrospun carbon nanofiber composite[144] Adapted with permission from ref. 142, 143 and 144 Copyright 2014 American Chemical Society

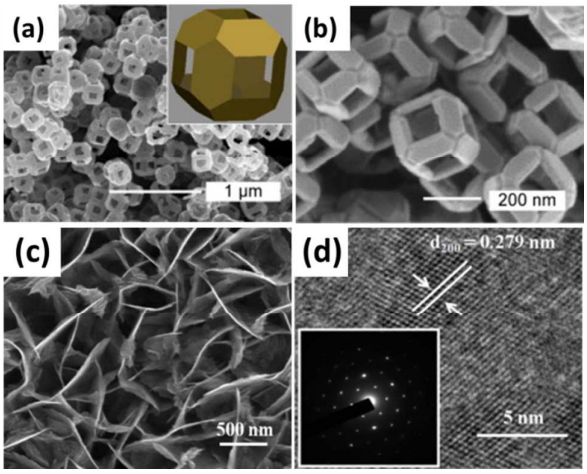

Fig. 12 (a-b) SEM images of skeletal $Cu_{1.75}S$ architecture, inset of (a) is simulated structure[150] (c-d) SEM images of $Cu_{1.8}S$ nanosheet arrays, inset of (d) is the SAED pattern[151] Adapted from Ref. 151 with permission from The Royal Society of Chemistry

employing this CE showed inferior PCE (mostly lower than 4%), the preferable stability and ease of fabrication made this CE a promising candidate for large-scale QDSSC production. CdS/CdSe QDSSC module with the aperture area of over 12 cm^2 have been fabricated, exhibiting a promising 2.31% PCE without cell performance degradation in 30 days (Fig. 10 presents the digital photo and performance of the module).[141]

6.1.2 Cu_xS

Despite the intensive studies employing Cu_2S as CE in QDSSC, it was reported that Cu_2S is a relatively unstable phase in its stoichiometric members, mainly due to the formation of Cu vacancies even in thermodynamic equilibrium with bulk copper metal.[145] It was even debated that the structural information on Cu_2S has been misled, since XRD analysis of the so called Cu_2S CE made by reacting brass with polysulfide solution revealed not Cu_2S, but $Cu_{1.75}S$.[146] Indeed, Cu_2S had already been found intrinsically unstable in previous experimental and theoretical investigations[125, 147], which could be attributed to its crystal structure behaving like a solid backbone of sulfur anions surrounded by a liquid of mobile Cu^+ cations.[148] It was also reported that Cu_2S easily degraded into Cu-deficient phases.[146] The misassignment of these Cu-deficient phases as Cu_2S due to their highly similar XRD patterns has also been stated in other copper sulfides application areas.[126] Thus, researchers turned their attention to the entire Cu_xS family, from Cu_2S (chalcocite) to CuS (covellite), $Cu_{1.96}S$ (djurleite), $Cu_{1.8}S$ (digenite), $Cu_{1.75}S$ (anilite) and $Cu_{1.12}S$ (yarrowite).

CuS, even though as a p-type semiconductor, exhibits mixed electronic and ionic conductivity due to the presence of Cu vacancies which give rise to free holes acting as electron acceptors.[149] The good stability and conductivity of CuS drive researchers to apply it as CE material in QDSSCs. Wang *et al.* developed a hierarchical CuS structure on conductive substrate by employing a one-step electrochemical deposition method (Fig. 11 a and b).[142] They monitored the overall performance of QDSSCs employing their CuS CE, brass-based Cu_2S CE and Pt CE under 120 min continuous illumination, respectively, among which the CuS CE showed best cell performance and stability.[142] Savariraj *et al.* prepared a knit coir mat structured CuS film directly on a FTO substrate applying the *in-situ* CBD method (Fig. 11 c).[152] They found that by varying the deposition time, the density of Cu vacancies increased, leading to enhanced CE performance.[152] Other structures of CuS including nano-flakes, nano-platelets and nano-peas[143, 153] were also prepared while novel materials like Mn-doped CuS[154], CuS/electrospun carbon nanofiber[144] CuS/reduced graphene oxide nanocomposite[155] and CuS/porous conductive substrate[156] (Fig. 11 d) were introduced to further optimize the performance of CuS based CEs.

Other Cu_xS materials also showed promising performance when employed in QDSSC. Chen *et al.* designed and developed a skeletal $Cu_{1.75}S$ nano-cage structure (Fig. 12 a and b).[157] The 3D opening hollow structure provided large surface area and facilitated electrolyte infiltration/diffusion, leading to enhanced QDSSC performance. A cyclic voltammetry measurement was further carried out to probe the redox processes and stability of the CEs. The higher current density and the super cyclability indicate that the novel $Cu_{1.7}S$ structure possesses preferable catalytic activity and stability compared to brass-based Cu_2S CE, as shown in Fig. 13. Ye *et al.* employed an *in situ* method to prepare $Cu_{1.8}S$ nanosheet arrays as CE for QDSSC (Fig. 12 c and d show the SEM pictures). A facial hydrothermal method was employed to prepare the porous structure utilizing CuCl and thiourea as precursors.[158]

Li *et al.* applied an *ex-situ* method to deposit a CuS/$Cu_{1.8}S$ composite material on FTO. CuS and $Cu_{1.8}S$ NPs were firstly prepared hydrothermally; followed by screen-printing on the conductive substrate.[131] They manipulated the Cu/S ratio and revealed that CuS shows a slightly superior performance than $Cu_{1.8}S$. The sintering temperature of Cu_xS coated FTO were also varied to optimized the CE performance. A highly reproducible efficiency of 6.28% was obtained for cells applying their CE.

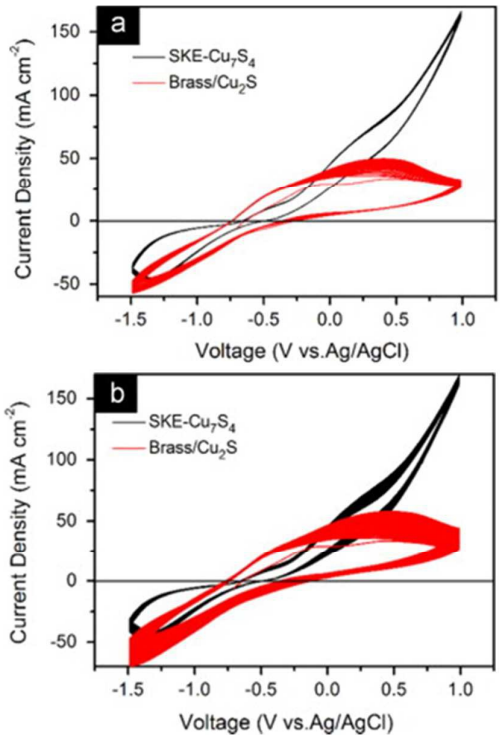

Fig. 13 Cyclic voltammograms of SKE-$Cu_{1.75}S$ and Brass/Cu_2S in 1 M/1M polysulfide solution (a) first 50 cycles and (b) 600 cycles[150]

Despite the intensive studies on Cu_xS materials, most of the reports focus on the development of electrocatalysts' novel nanostructuring or facile synthesis routes. Less attention is paid regarding the intrinsic electrochemical properties of Cu_xS. Considering the various compositions available for copper sulfides, a systemic investigation on their optical and electrochemical properties is necessary. Kim *et al.* developed a novel CBD method to deposit Cu_xS films on FTO substrates.[146]

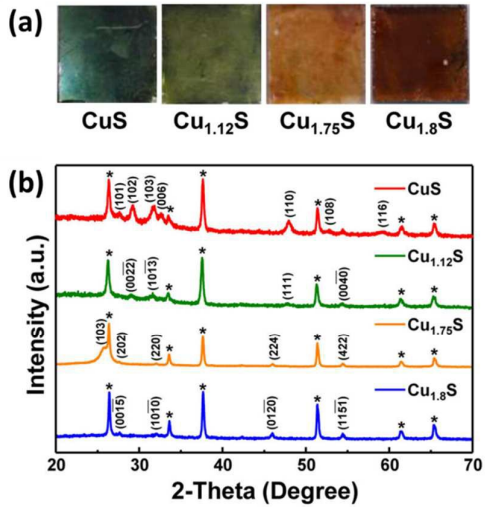

Fig. 14 (a) Photographs and (b) XRD patterns (peaks from the FTO substrate are marked with asterisks) of copper sulfides: CuS, $Cu_{1.12}S$, $Cu_{1.75}S$, and $Cu_{1.8}S$[146] Reprint with permission from ref. 146 Copyright 2012 American Chemical Society

By varying the concentration ratio of the precursors, Cu_xS with various stoichiometries were obtained, allowing a systemic study of the composition-dependent electrocatalytic activity of Cu_xS (Fig. 14 present the digital photos and XRD patterns of copper sulfides). Results indicated that when applying different kinds of Cu_xS materials as CE in QDSSCs, CuS possesses superior performance compared to other Cu_xS. Tafel polarization and Nyquist plots obtained using symmetric dummy cells ascertained that the catalytic ability of Cu_xS films shows a decreasing trend as the amount of Cu in the Cu_xS films became progressively richer, as presented in Fig. 15. More interestingly, the stability of Cu_xS films was also relevant to their composition. Generally, the Cu-deficient films (CuS and $Cu_{1.12}S$) were more stable than the Cu-rich counterparts ($Cu_{1.75}S$ and $Cu_{1.8}S$), due to their greater resistance against surface oxidation.

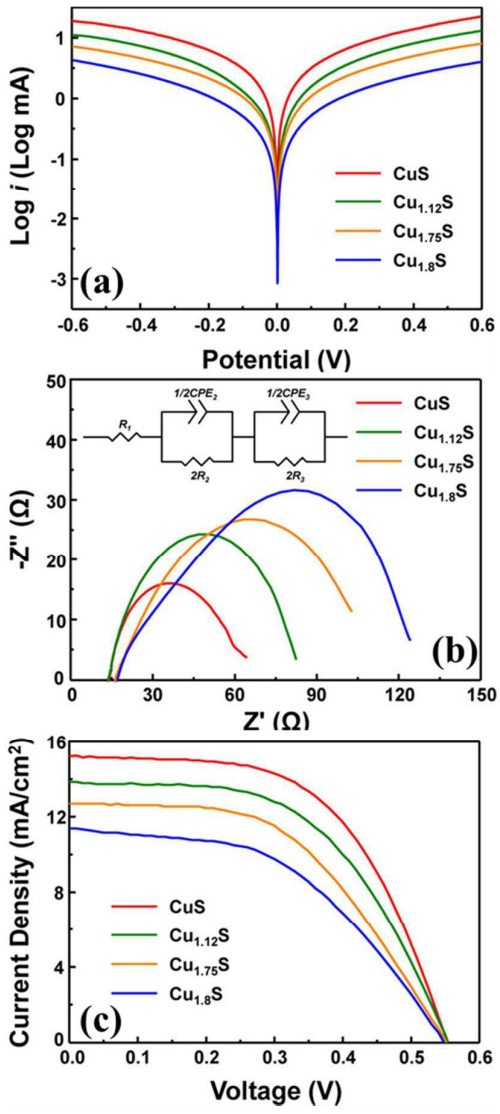

Fig. 15 (a) Tafel polarization curves (b) Nyquist plots of Cu_xS (inset shows an equivalent circuit) and (c) J–V curves of QDSSCs with various Cu_xS CEs under 1 sun illumination[146] Reprint with permission from ref. 146 Copyright 2012 American Chemical Society

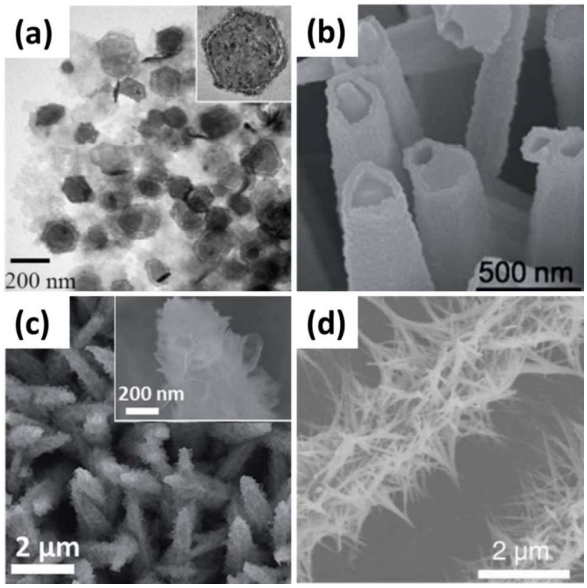

Fig. 16 SEM images of (a) cobalt sulfide core–shell nanosheet structure[159] (b) Carbon fiber/CoS nanotube arrays hybrid structure[160] (c) CoS nanorod arrays/graphite paper composite[161] and (d) CoS nanowires/Au hybridized network[162] (b) and (c) are adapted from Ref. 160 and 161 with permission from The Royal Society of Chemistry

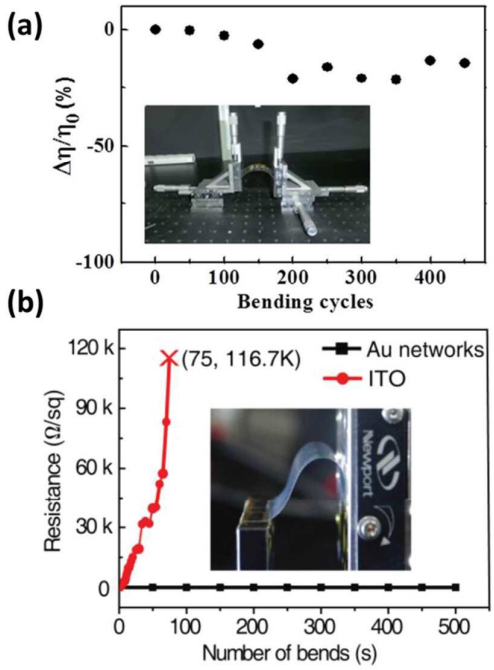

Fig. 17 (a) Mechanical robust testing of the QDSSCs employing CoS nanorod arrays/graphite paper as CE, where $\Delta\eta/\eta_0$ is the function of mechanical bending cycles[161] and (b) variations in resistance of an CoS-Au network electrode and an ITO electrode on PET film as a function of the number of bending cycles[162], insets of a and b show the bending setups (a) is adapted from Ref. 161 with permission from The Royal Society of Chemistry

6.2 Other metal sulfides

Other metal sulfides, including cobalt sulfide, lead sulfide, nickel sulfide and iron sulfide are also tested as CE material in QDSSC.[163-168] Among them, CoS and PbS showed promising catalytic ability.

Yang *et al.* prepared a low cost CoS CE for CdS/CdSe QDSSC employing a CBD method.[164] According to their results, the electrocatalytic activities of the sulfide electrodes followed the order of CuS＞CoS＞NiS＞Pt, however, CuS showed inferior stability. It was also argued that the greater reflectance of the CoS electrode enabled efficient reflection of the incident light on the TiO_2 layer leading to more efficient sun light absorption. The same group further designed and investigated cobalt sulfide core–shell nanosheet structure (Fig. 16 a)[159] and CuS/CoS hybrid material[169] to obtain more catalytic and stable CE. Yuan *et al.* developed an electrodeposition method to deposit CoS film on conductive substrate[170]; they showed that the electrodeposited CoS/ITO CE offered remarkable electrocatalytic activity compared to CBD CoS/ITO or CoS/FTO CE. Flexible CoS-containing CEs were also fabricated to functionalize flexible QDSSCs. Carbon fiber/CoS nanotube arrays hybrid structures (Fig. 16 b)[160], CoS nanorod arrays/graphite paper composite (Fig. 16 c)[161] and CoS nanowires/Au hybridized networks (Fig. 16 d)[162] were subtly designed and prepared as efficient flexible CE architectures. Those CEs exhibited dramatic catalytic activity and superior mechanical strength. No obvious changes in morphology and catalytic ability were observed after bending tests, as indicated in Fig. 17.

Tachan *et al.* introduced a PbS CE for QDSSC.[163] The PbS CE was fabricated by immersing Pb foil in H_2SO_4 firstly, followed by polysulfide treatment. In their study, charge transfer resistance of the PbS electrode in aqueous polysulfide electrolyte was calculated and when compared to alternative CE materials for polysulfide electrolyte, PbS showed the minimum R_{ct} value of all. Stability tests of the PbS counter electrode showed no degradation under illumination when in contact with polysulfide electrolyte for over 100 h. The PbS material was further composited with carbon black[171] or graphene[172], aiming at obtaining more efficient and stable CE. The R_{ct} of the composite CE was calculated to be less than 10 Ω cm^2, which is an order of magnitude lower than the value obtained in the study on pure PbS CE. Other composite materials, including PbS/CuS[173] and PbS/ZnO nanorod core-shell materials[174] were further designed and investigated as promising PbS-containing CE for QDSSC.

Earth-abundant metal pyrites (FeS_2, CoS_2, NiS_2, and their alloys) thin films were also systemically investigated as alternative electrocatalysts for polysulfide reduction.[175] CV and EIS results demonstrated the high catalytic activity of the transition metal pyrites toward polysulfide reduction and highlighted the particularly high intrinsic activity of NiS_2, which could realize improved QDSSC performance, as shown in Fig. 18. Furthermore, alloying different transition metal pyrites could introduce structural disorders, which increase their areal density of active sites for catalysis, leading to enhanced performance.

Ternary and quaternary chalcogenides, normally regarded as attractive light absorbing materials in PV cells, were also introduced as CE material in QDSSCs, due to their good

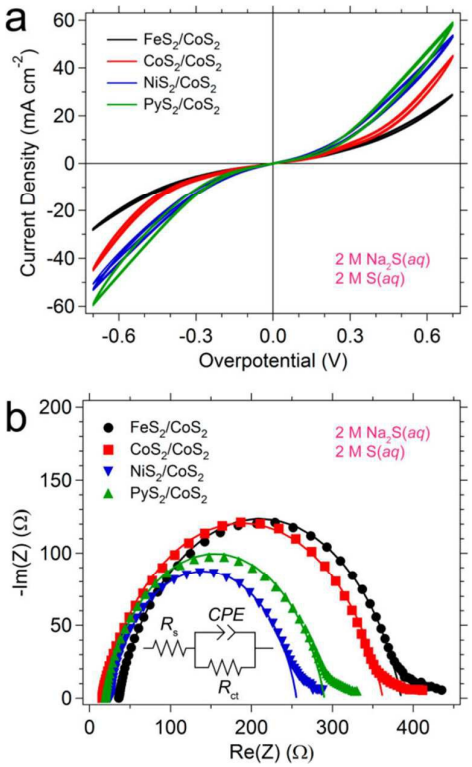

Fig. 18 (a) CV and (b) EIS characterization of the symmetrical cells of the metal pyrites thin films prepared on CoS_2/glass electrodes toward polysulfide reduction, inset of b shows the equivalent circuit, the results of these fittings shown as solid line traces[175] Reprint with permission from ref. 175 Copyright 2014 American Chemical Society

stability and catalytic ability towards the aqueous polysulfide electrolyte. Non-toxic and low-cost materials like $CuInS_2$ or Cu_2ZnSnS_4 (CZTS) CE were successfully incorporated in QDSSCs and exhibited promising performance.[176-181]

6.3. Metal Selenides

As an important class of chalcogenides, semiconducting selenides have drawn enormous attention due to their distinctive electronic properties and interesting chemical behaviors. It has been investigated in a wide variety of potential applications, such as optical recording materials, sensor, laser materials and PV fields.[182-185] Quite recently, metal selenides emerge as a new class of CE electrocatalysts for QDSSCs, despite its conventional and successful utilization as sensitizers for photo-electrodes. Choi *et al.* conducted a thorough study on binary metal selenide materials and assessed their feasibility as CE material for QDSSCs.[186] Eight different types of binary selenides (MnSe, $CoSe_2$, $NiSe_2$, $Cu_{1.8}Se$, $MoSe_2$, WSe_2, PbSe, and Bi_2Se_3) were randomly selected as electro-catalyst candidates and employed to prepare CEs for QDSSCs. The performance of solar cells featuring these metal selenides was compared with that of QDSSC employing conventional Pt CE. The recorded J-V curves (Fig. 19) reveal that solar cell devices involving $Cu_{1.8}Se$ or PbSe CE showed better overall performance than that with Pt, while inferior performances were obtained when applying other CEs. An in-

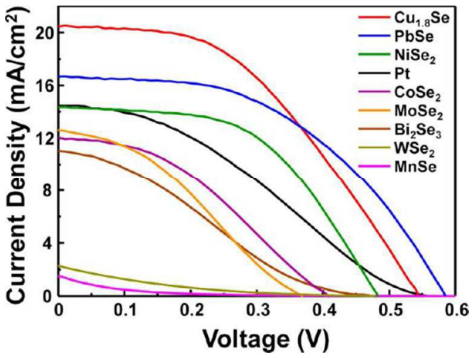

Fig. 19 J–V curves of QDSSCs with various metal selenide CEs under 1 sun illumination[186] Reprint with permission from ref. 186 Copyright 2014 American Chemical Society

depth study on $Cu_{1.8}Se$ and PbSe CE was further conducted to investigate their physical and electrochemical properties. XRD, Raman and XPS results ascertained their chemical compositions and revealed their air stability (Fig. 20 highlighted XPS spectra of $Cu_{1.8}Se$ and PbSe film, respectively). Specifically, $Cu_{1.8}S$ has a favorable stability while PbSe was partly oxidized to PbO and SeO_2 due to its instability under air. EIS results revealed that $Cu_{1.8}Se$, compared to PbSe, had better catalytic ability and electrochemical stability when functioning in the polysulfide electrolyte. A maximized PCE of 5.01% was obtained for QDSSCs using $Cu_{1.8}Se$ CE. However, the CEs were prepared using a SILAR method in this study, making it difficult to control the metal selenides films' crystallinity, grain size or composition. These parameters subtly dictate the resulting films' physicochemical properties. Thus, there is still much room for the improvement of metal selenides CE's performance.

Bo *et al.* developed a facial approach to fabricate copper selenide CE.[187] A red layer of Se was firstly deposited on the

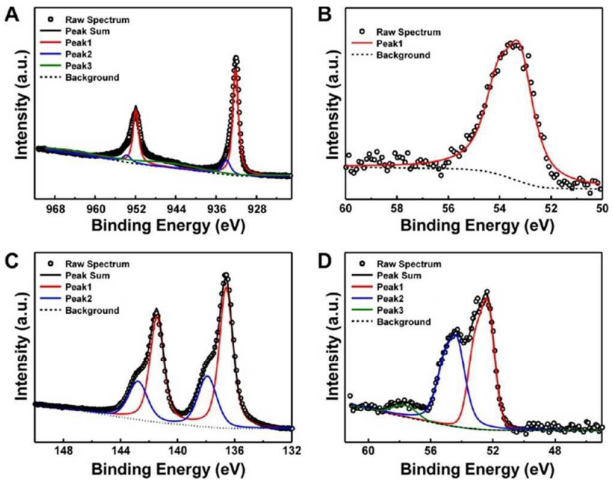

Fig. 20 XPS spectra of (a) Cu 2p (peak 1, Cu^+ from $Cu_{1.8}Se$; peak 2, Cu^{2+} from $Cu_{1.8}Se$; peak 3, shake-up satellites due to Cu^+) (b) Se 3d from the $Cu_{1.8}Se$ film (c) Pb 4f (peak 1, Pb^{2+} from PbSe; peak 2, Pb^{2+} from PbO) and (d) Se 3d (peak 1, Se^{2-} from PbSe; peak 2, intermediate oxidation state (roughly corresponding to Se^0); peak 3, Se^{4+} from SeO_2) from the PbSe film[186] Reprint with permission from ref. 186 Copyright 2014 American Chemical Society

conductive substrate, followed by a simple Cu^{2+} treatment. This method was reported as easy-processing and time-saving, while it eliminated the rigorous preparing conditions. This method also allowed the preparation of other metal selenide functional CEs, such as PbSe, Ag_2Se, etc. However, the resulting copper selenide film consisted of the stoichiometries of Cu_3Se_2 and $Cu_{1.8}Se$ while traces of selenium oxide were observed. This might degrade the electrochemical property of the copper selenide film, as indicated by the lower PCE of QDSSC obtained (lower than 4%). Liu *et al.* reported a low-temperature, solution-based method to deposit metal selenide films as efficient CE for QDSSC.[188] The metal selenide films were formed by drop casting their dissolved inks onto a conductive substrate, followed by a mild thermal treatment. $FeSe_2$, $Cu_{1.8}S$, and CuSe films have been prepared using this method, all of which showed promising performance. This facial preparation method offers great potential for low-cost and large-scale production of the metal selenides materials for solar cell application.

Chen *et al.* designed and developed $Cu_{2-x}Se$ nanotubes with hierarchical architecture as efficient CE for QDSSC.[189] The 1-dimensional hollow nanostructure consisting of flower like surface (as indicated by SEM and TEM images shown in Fig. 21) was prepared using a solution based *ex-situ* method under room temperature, employing Cu nanotube as an intermediate product. The unique morphology of the copper selenide nanotubes provides favorable catalytic ability and electrical conductivity while the ease of fabrication enables wider application. QDSSCs exhibited PCE as high as 6.25% when applying this nanotube-based CE. The size and composition of the copper selenides were further manipulated by Bai *et al.* to optimize the performance of QDSSC. The non-stoichiometric $Cu_{2-x}Se$ was employed since the conductivity could be improved by partial oxidization of exactly stoichiometric Cu_2Se. The superior property of the copper selenide CEs, together with their unique porous titania nanohybrids photoelectrode structure, boosted the PCE of QDSSC up to 7.11%.[21]

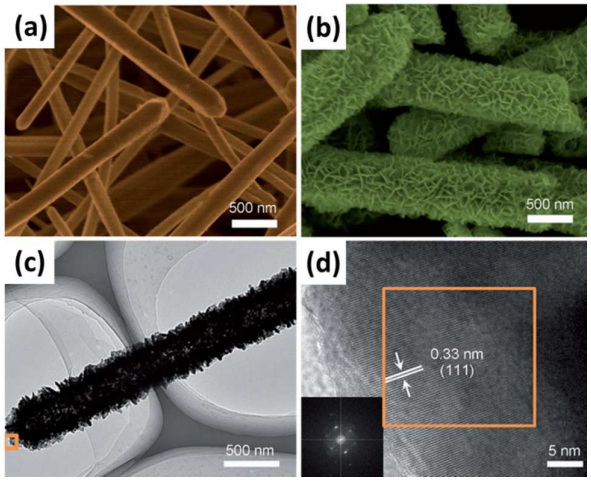

Fig. 21 Field-emission SEM (FESEM) images of the (a) Cu nanowires and (b) $Cu_{2-x}Se$ nanotubes (c-d) TEM images of the nanotubes, inset of (d) is fast Fourier transforms (FFT) of the HRTEM images of the selected areas in (c)[189]

Considering the encouraging performance of metal selenides as CE material for QDSSC, the on-going studies on this class of material seem inadequate.[190-192] The development of more efficient CE for QDSSCs could be feasible based on further investigation in metal selenide materials.

7. Conclusions and prospects

The power conversion efficiency of QDSSC exhibited steady growth over the years due to numerous and widespread efforts made in this area, even though it is still in the shade compared to other new generation solar cell devices, such as DSSC, organic solar cells and the newly emerged perovskite solar cells, where the use of Pb compounds is a serious concern. A critical factor to boost the QDSSC efficiency is to build a compatible electrolyte-CE system. S^{2-}/S_n^{2-} redox electrolyte has been proved as an efficient charge mediator for QDSSC. Thus, it is of vital importance to develop a CE better functionalizing the polysulfide electrolyte. Recently, a large number of studies have been reported focusing on the investigation of efficient CE materials for QDSSCs. Noble metal like Pt or Au was not compatible with polysulfide electrolyte due to the fact that adsorption of sulfur-containing compound on the surface, which degrades its electro-catalytic ability. Carbon material, in which though no degradation was observed, showed intrinsically lower catalytic property towards the reduction of S_n^{2-}. Metal chalcogenides, including metal sulfides and metal selenides, exhibited superior catalytic ability and stability in polysulfide electrolyte, among which Cu and Co based materials showed extremely promising performances. Carefully prepared compositional or morphological manipulations of the metal chalcogenide materials have dramatically improved its electrocatalytic properties. These novel CE materials were successfully employed in QDSSCs resulting in devices with enhanced efficiency and stability.

In spite of the progresses made in this area, the development of high efficiency QDSSC featuring metal chalcogenide CEs is still in the primary stage. To further develop this field, a series of experimental and theoretical issues are to be considered and addressed. The catalytic ability and conductivity of the metal chalcogenide materials could be further improved, by providing higher surface areas (for more reaction sites), unique architectures (for the ease of electrolyte penetration and facile electro-catalysis) or hybridizing with other catalytic/conductive materials (synergetic functionalization). The stability issue of the metal chalcogenide materials, including mechanical stability and electrochemical stability, should be seriously considered and approaches like employing novel material preparation methods or constructing unique material micro-structures might be required to solve the problems. A fundamental understanding of the relationship between the metal chalcogenides material structure and their electrochemical characteristics is necessary to direct the optimization of the synthesis parameters and material properties. Furthermore, efforts to develop low-toxic, earth-abundant raw materials and low-cost, large-area, green

manufacturing processes for metal chalcogenides should be taken as well to guarantee that the development in this area fulfil the basic commercial and environmental requirements. Thus, the investigation and application of novel metal chalcogenides QDSSC CE materials is a quite challenging yet promising research topic, which provides opportunity for the further improvement of the QDSSC performance and for its potential commercialization.

Acknowledgements

G. Chen acknowledges the support from the National Natural Science Foundation of China (11375256) and Science and Technology Commission of Shanghai Municipality (14JC1493300). K.R. Thampi acknowledges the SFI-Airtricity Stokes professorship grant [S07/EN/E013].

References

1. J. P. Holdren, *Science*, 2008, 319, 424-434.
2. N. S. Lewis, *science*, 2007, 315, 798-801.
3. M. Graetzel, R. A. J. Janssen, D. B. Mitzi and E. H. Sargent, *Nature*, 2012, 488, 304-312.
4. H. Savin, P. Repo, G. von Gastrow, P. Ortega, E. Calle, M. Garín and R. Alcubilla, *Nature Nanotech.* , 2015, 10, 624-628.
5. J. Kim, Z. Hong, G. Li, T.-b. Song, J. Chey, Y. S. Lee, J. You, C.-C. Chen, D. K. Sadana and Y. Yang, *Nature Commun.*, 2015, 6.
6. Y. Yang, W. Chen, L. Dou, W.-H. Chang, H.-S. Duan, B. Bob, G. Li and Y. Yang, *Nature Photon.*, 2015, 9, 190-198.
7. B. O'regan and M. Grätzel, *Nature*, 1991, 353, 737-740.
8. M. Grätzel, *Inorg. Chem.*, 2005, 44, 6841-6851.
9. M. Grätzel, *J. Photochem. Photobiol. A*, 2004, 164, 3-14.
10. M. Grätzel, *J. Photochem. Photobiol. C*, 2003, 4, 145-153.
11. S. Rühle, M. Shalom and A. Zaban, *ChemPhysChem*, 2010, 11, 2290-2304.
12. I. Mora-Sero, S. Gimenez, F. Fabregat-Santiago, R. Gomez, Q. Shen, T. Toyoda and J. Bisquert, *Acc. Chem. Res.*, 2009, 42, 1848-1857.
13. A. Nozik, *Phys. E*, 2002, 14, 115-120.
14. P. V. Kamat, *J. Phys. Chem. C*, 2008, 112, 18737-18753.
15. S. Mathew, A. Yella, P. Gao, R. Humphry-Baker, B. F. Curchod, N. Ashari-Astani, I. Tavernelli, U. Rothlisberger, M. K. Nazeeruddin and M. Grätzel, *Nature Chem.*, 2014, 6, 242-247.
16. M. Reed, J. Randall, R. Aggarwal, R. Matyi, T. Moore and A. Wetsel, *Physical Review Letters*, 1988, 60, 535.
17. W. K. Leutwyler, S. L. Bürgi and H. Burgl, *Science*, 1996, 271, 933-937.
18. O. E. Semonin, J. M. Luther, S. Choi, H.-Y. Chen, J. Gao, A. J. Nozik and M. C. Beard, *Science*, 2011, 334, 1530-1533.
19. K. Zhao, Z. Pan, I. Mora-Seró, E. Cánovas, H. Wang, Y. Song, X. Gong, J. Wang, M. Bonn and J. Bisquert, *J. Am. Chem. Soc.*, 2015, 137, 5602-5609.
20. S. Jiao, Q. Shen, I. Mora-Seró, J. Wang, Z. Pan, K. Zhao, Y. Kuga, X. Zhong and J. Bisquert, *ACS Nano*, 2015, 9, 908-915.
21. Y. Bai, C. Han, X. Chen, H. Yu, X. Zong, Z. Li and L. Wang, *Nano Energy*, 2015, 13, 609-619.
22. Z. Pan, I. n. Mora-Seró, Q. Shen, H. Zhang, Y. Li, K. Zhao, J. Wang, X. Zhong and J. Bisquert, *J. Am. Chem. Soc.*, 2014, 136, 9203-9210.
23. J. Tian, L. Lv, C. Fei, Y. Wang, X. Liu and G. Cao, *J. Mater. Chem. A*, 2014.
24. H. McDaniel, N. Fuke, N. S. Makarov, J. M. Pietryga and V. I. Klimov, *Nature Commun.*, 2013, 4.
25. E. M. Barea, M. Shalom, S. Giménez, I. Hod, I. Mora-Seró, A. Zaban and J. Bisquert, *J. Am. Chem. Soc.*, 2010, 132, 6834-6839.
26. M. Shalom, S. Ruhle, I. Hod, S. Yahav and A. Zaban, *J. Am. Chem. Soc.*, 2009, 131, 9876-9877.
27. T.-L. Li, Y.-L. Lee and H. Teng, *Energy Environ. Sci.*, 2012, 5, 5315-5324.
28. P. V. Kamat, *Acc. Chem. Res.*, 2012, 45, 1906-1915.
29. N. Fuke, L. B. Hoch, A. Y. Koposov, V. W. Manner, D. J. Werder, A. Fukui, N. Koide, H. Katayama and M. Sykora, *Acs Nano*, 2010, 4, 6377-6386.
30. Z. Pan, K. Zhao, J. Wang, H. Zhang, Y. Feng and X. Zhong, *ACS Nano*, 2013, 7, 5215-5222.
31. J. Wang, I. Mora-Seró, Z. Pan, K. Zhao, H. Zhang, Y. Feng, G. Yang, X. Zhong and J. Bisquert, *J. Am. Chem. Soc.*, 2013, 135, 15913-15922.
32. O. Niitsoo, S. K. Sarkar, C. Pejoux, S. Rühle, D. Cahen and G. Hodes, *J. Photochem. Photobiol. A*, 2006, 181, 306-313.
33. H. Zhang, K. Cheng, Y. Hou, Z. Fang, Z. Pan, W. Wu, J. Hua and X. Zhong, *Chem. Commun.*, 2012, 48, 11235-11237.
34. A. Salant, M. Shalom, I. Hod, A. Faust, A. Zaban and U. Banin, *Acs Nano*, 2010, 4, 5962-5968.
35. T. P. Brennan, P. Ardalan, H. B. R. Lee, J. R. Bakke, I. Ding, M. D. McGehee and S. F. Bent, *Adv. Energy Mater.*, 2011, 1, 1169-1175.
36. H. Lee, M. Wang, P. Chen, D. R. Gamelin, S. M. Zakeeruddin, M. Gratzel and M. K. Nazeeruddin, *Nano Lett.*, 2009, 9, 4221-4227.
37. H. Lee, H. C. Leventis, S. J. Moon, P. Chen, S. Ito, S. A. Haque, T. Torres, F. Nüesch, T. Geiger and S. M. Zakeeruddin, *Adv. Funct. Mater.*, 2009, 19, 2735-2742.
38. I. Robel, V. Subramanian, M. Kuno and P. V. Kamat, *J. Am. Chem. Soc.*, 2006, 128, 2385-2393.
39. P. Brown and P. V. Kamat, *J. Am. Chem. Soc.*, 2008, 130, 8890-8891.
40. X.-Y. Yu, J.-Y. Liao, K.-Q. Qiu, D.-B. Kuang and C.-Y. Su, *Acs Nano*, 2011, 5, 9494-9500.
41. P. K. Santra and P. V. Kamat, *J. Am. Chem. Soc.*, 2012, 134, 2508-2511.
42. C. Li, L. Yang, J. Xiao, Y.-C. Wu, M. Søndergaard, Y. Luo, D. Li, Q. Meng and B. B. Iversen, *Phys. Chem. Chem.*, 2013, 15, 8710-8715.
43. X. Huang, S. Huang, Q. Zhang, X. Guo, D. Li, Y. Luo, Q. Shen, T. Toyoda and Q. Meng, *Chem. Commun.*, 2011, 47, 2664-2666.
44. H. Zhang, Y. Wang, D. Yang, Y. Li, H. Liu, P. Liu, B. J. Wood and H. Zhao, *Adv. Mater.*, 2012, 24, 1598-1603.
45. H. Zhang, Y. Li, Y. Wang, P. Liu, H. Yang, X. Yao, T. An, B. J. Wood and H. Zhao, *J. Mater. Chem. A*, 2013, 1, 6563-6571.
46. L.-B. Li, Y.-F. Wang, H.-S. Rao, W.-Q. Wu, K.-N. Li, C.-Y. Su and D.-B. Kuang, *ACS Appl. Mater. Interfaces*, 2013, 5, 11865-11871.
47. K. Meng, P. K. Surolia and K. R. Thampi, *J. Mater. Chem. A*, 2014, 2, 10231-10238.

48. P. Sudhagar, T. Song, D. H. Lee, I. Mora-Seró, J. Bisquert, M. Laudenslager, W. M. Sigmund, W. I. Park, U. Paik and Y. S. Kang, *J. Phys. Chem. Lett.*, 2011, 2, 1984-1990.
49. J. Hensel, G. Wang, Y. Li and J. Z. Zhang, *Nano Lett.*, 2010, 10, 478-483.
50. K. S. Leschkies, R. Divakar, J. Basu, E. Enache-Pommer, J. E. Boercker, C. B. Carter, U. R. Kortshagen, D. J. Norris and E. S. Aydil, *Nano Lett.*, 2007, 7, 1793-1798.
51. K. Meng, P. K. Surolia, O. Byrne and K. R. Thampi, *J. Power Sources*, 2014, 248, 218-223.
52. J. Jean, S. Chang, P. R. Brown, J. J. Cheng, P. H. Rekemeyer, M. G. Bawendi, S. Gradečak and V. Bulović, *Adv. Mater.*, 2013, 25, 2790-2796.
53. J. Tian, Q. Zhang, E. Uchaker, Z. Liang, R. Gao, X. Qu, S. Zhang and G. Cao, *J. Mater. Chem. A*, 2013, 1, 6770-6775.
54. T. You, L. Jiang, K.-L. Han and W.-Q. Deng, *Nanotechnology*, 2013, 24, 245401.
55. M. Seol, H. Kim, Y. Tak and K. Yong, *Chem. Commun.*, 2010, 46, 5521-5523.
56. S. Huang, Q. Zhang, X. Huang, X. Guo, M. Deng, D. Li, Y. Luo, Q. Shen, T. Toyoda and Q. Meng, *Nanotechnology*, 2010, 21, 375201.
57. H. Wang, M. Miyauchi, Y. Ishikawa, A. Pyatenko, N. Koshizaki, Y. Li, L. Li, X. Li, Y. Bando and D. Golberg, *J. Am. Chem. Soc.*, 2011, 133, 19102-19109.
58. T. Toyoda and Q. Shen, *J. Phys. Chem. Lett.*, 2012, 3, 1885-1893.
59. J. Chen, C. Li, G. Eda, Y. Zhang, W. Lei, M. Chhowalla, W. I. Milne and W.-Q. Deng, *Chem. Commun.*, 2011, 47, 6084-6086.
60. Y.-L. Lee and C.-H. Chang, *J. Power Sources*, 2008, 185, 584-588.
61. A. J. Haring, M. E. Pomatto, M. R. Thornton and A. J. Morris, *ACS Appl. Mater. Interfaces*, 2014, 6, 15061-15067.
62. H. J. Lee, P. Chen, S.-J. Moon, F. Sauvage, K. Sivula, T. Bessho, D. R. Gamelin, P. Comte, S. M. Zakeeruddin and S. I. Seok, *Langmuir*, 2009, 25, 7602-7608.
63. Y. Tachibana, H. Y. Akiyama, Y. Ohtsuka, T. Torimoto and S. Kuwabata, *Chem. Lett.*, 2007, 36, 88-89.
64. K. Meng and K. R. Thampi, *ACS Appl. Mater. Interfaces*, 2014, 6, 20768-20775.
65. K. Meng, P. K. Surolia, O. Byrne and K. R. Thampi, *J. Power Sources*, 2015, 275, 681-687.
66. H. J. Lee, J.-H. Yum, H. C. Leventis, S. M. Zakeeruddin, S. A. Haque, P. Chen, S. I. Seok, M. Grätzel and M. K. Nazeeruddin, *J. Phys. Chem. C*, 2008, 112, 11600-11608.
67. L. Li, X. Yang, J. Gao, H. Tian, J. Zhao, A. Hagfeldt and L. Sun, *J. Am. Chem. Soc.*, 2011, 133, 8458-8460.
68. I. Hod and A. Zaban, *Langmuir*, 2013, 30, 7264-7273.
69. J. Duan, H. Zhang, Q. Tang, B. He and L. Yu, *J. Mater. Chem. A*, 2015, 3, 17497-17510.
70. I. Hwang and K. Yong, *ChemElectroChem*, 2015.
71. H. Jun, M. Careem and A. Arof, *Renew. Sust. Energ. Rev.*, 2013, 22, 148-167.
72. M. Kouhnavard, S. Ikeda, N. Ludin, N. A. Khairudin, B. Ghaffari, M. Mat-Teridi, M. Ibrahim, S. Sepeai and K. Sopian, *Renew. Sust. Energ. Rev.*, 2014, 37, 397-407.
73. P. V. Kamat, *J. Phys. Chem. Lett.*, 2013, 4, 908-918.
74. M. Wu, X. Lin, Y. Wang and T. Ma, *J. Mater. Chem. A*, 2015, DOI: 10.1039/C5TA03682H.
75. Z. Yang, C.-Y. Chen, P. Roy and H.-T. Chang, *Chem. Commun.*, 2011, 47, 9561-9571.
76. A. Yella, H.-W. Lee, H. N. Tsao, C. Yi, A. K. Chandiran, M. K. Nazeeruddin, E. W.-G. Diau, C.-Y. Yeh, S. M. Zakeeruddin and M. Grätzel, *Science*, 2011, 334, 629-634.
77. C. H. Chang and Y. L. Lee, *Appl. Phys. Lett.*, 2007, 91, 053503 - 053503-053503.
78. M. Shalom, S. Dor, S. Ruhle, L. Grinis and A. Zaban, *J. Phys. Chem. C*, 2009, 113, 3895-3898.
79. A. Fujishima, E. Sugiyama and K. Honda, *Bull. Chem. Soc. Japan*, 1971, 44, 304-304.
80. H. Gerischer, *J. Electroanal. Chem. Interfac.*, 1975, 58, 263-274.
81. K. Rajeshwar, P. Singh and J. DuBow, *Electrochim. Acta*, 1978, 23, 1117-1144.
82. Miller, B. Amp and A. Heller, *Nature*, 1976, 262, 680.
83. A. B. Ellis, S. W. Kaiser and M. S. Wrighton, *J. Am. Chem. Soc.*, 1976, 98, 1635-1637.
84. G. Hodes, J. Manassen and D. Cahen, *Nature*, 1976, 261, 403.
85. V. Chakrapani, D. Baker and P. V. Kamat, *J. Am. Chem. Soc.*, 2011, 133, 9607-9615.
86. M. A. Hossain, J. R. Jennings, C. Shen, J. H. Pan, Z. Y. Koh, N. Mathews and Q. Wang, *J. Mater. Chem.*, 2012, 22, 16235-16242.
87. J.-W. Lee, D.-Y. Son, T. K. Ahn, H.-W. Shin, I. Y. Kim, S.-J. Hwang, M. J. Ko, S. Sul, H. Han and N.-G. Park, *Sci. Rep.*, 2013, 3.
88. S. Do Sung, I. Lim, P. Kang, C. Lee and W. I. Lee, *Chem. Commun.*, 2013, 49, 6054-6056.
89. C.-Y. Chou, C.-P. Lee, R. Vittal and K.-C. Ho, *J. Power Sources*, 2011, 196, 6595-6602.
90. V. Jovanovski, V. González-Pedro, S. Giménez, E. Azaceta, G. n. Cabañero, H. Grande, R. Tena-Zaera, I. n. Mora-Seró and J. Bisquert, *J. Am. Chem. Soc.*, 2011, 133, 20156-20159.
91. J. Qian, Q.-S. Liu, G. Li, K.-J. Jiang, L.-M. Yang and Y. Song, *Chem. Commun.*, 2011, 47, 6461-6463.
92. Z. Yu, Q. Zhang, D. Qin, Y. Luo, D. Li, Q. Shen, T. Toyoda and Q. Meng, *Electrochem. Commun.*, 2010, 12, 1776-1779.
93. C.-F. Chi, P. Chen, Y.-L. Lee, I.-P. Liu, S.-C. Chou, X.-L. Zhang and U. Bach, *J. Mater. Chem.*, 2011, 21, 17534-17540.
94. G. Larramona, C. Choné, A. Jacob, D. Sakakura, B. Delatouche, D. Péré, X. Cieren, M. Nagino and R. Bayón, *Chem. Mater.*, 2006, 18, 1688-1696.
95. S. Gimenez, I. Mora-Sero, L. Macor, N. Guijarro, T. Lana-Villarreal, R. Gomez, L. J. Diguna, Q. Shen, T. Toyoda and J. Bisquert, *Nanotechnology*, 2009, 20, 295204.
96. L. T. L. Lee, J. He, B. Wang, Y. Ma, K. Y. Wong, Q. Li, X. Xiao and T. Chen, *Sci. Rep.*, 2014, 4.
97. G. r. Li, F. Wang, Q. w. Jiang, X. p. Gao and P. w. Shen, *Angew. Chem. Int. Ed.*, 2010, 49, 3653-3656.
98. I. Hwang and K. Yong, *ChemElectroChem*, 2015, 2, 634-653.
99. S. Thomas, T. Deepak, G. Anjusree, T. Arun, S. V. Nair and A. S. Nair, *J. Mater. Chem. A*, 2014, 2, 4474-4490.
100. Y. L. Lee and Y. S. Lo, *Adv. Funct. Mater.*, 2009, 19, 604-609.
101. J. G. Radich, R. Dwyer and P. V. Kamat, *J. Phys. Chem. Lett.*, 2011, 2, 2453-2460.

102. X.-Y. Yu, B.-X. Lei, D.-B. Kuang and C.-Y. Su, *Chem. Sci.*, 2011, 2, 1396-1400.
103. T. Kiyonaga, T. Akita and H. Tada, *Chem. Commun.*, 2009, 2011-2013.
104. G. Zhu, L. Pan, H. Sun, X. Liu, T. Lv, T. Lu, J. Yang and Z. Sun, *ChemPhysChem*, 2012, 13, 769-773.
105. Y.-P. Yoon, J.-H. Kim, S.-H. Kang, H. Kim, C.-J. Choi, K.-K. Kim and K.-S. Ahn, *Appl. Phys. Lett.*, 2014, 105, 083116.
106. H. Zhu, J. Wei, K. Wang and D. Wu, *Sol. Energy Mater. Sol. Cells*, 2009, 93, 1461-1470.
107. J. D. Roy-Mayhew, D. J. Bozym, C. Punckt and I. A. Aksay, *Acs Nano*, 2010, 4, 6203-6211.
108. D. Chen, H. Zhang, Y. Liu and J. Li, *Energy Environ. Sci.*, 2013, 6, 1362-1387.
109. M. Wu, X. Lin, T. Wang, J. Qiu and T. Ma, *Energy Environ. Sci.*, 2011, 4, 2308-2315.
110. J. Chen, K. Li, Y. Luo, X. Guo, D. Li, M. Deng, S. Huang and Q. Meng, *Carbon*, 2009, 47, 2704-2708.
111. W. J. Lee, E. Ramasamy, D. Y. Lee and J. S. Song, *ACS Appl. Mater. Interfaces*, 2009, 1, 1145-1149.
112. P. Joshi, Y. Xie, M. Ropp, D. Galipeau, S. Bailey and Q. Qiao, *Energy Environ. Sci.*, 2009, 2, 426-429.
113. H. Sun, Y. Luo, Y. Zhang, D. Li, Z. Yu, K. Li and Q. Meng, *J. Phys. Chem. C*, 2010, 114, 11673-11679.
114. Q. Zhang, Y. Zhang, S. Huang, X. Huang, Y. Luo, Q. Meng and D. Li, *Electrochem. Commun.*, 2010, 12, 327-330.
115. G. Hodes, J. Manassen and D. Cahen, *J. Electrochem. Soc.*, 1980, 127, 544-549.
116. S.-Q. Fan, B. Fang, J. H. Kim, J.-J. Kim, J.-S. Yu and J. Ko, *Appl. Phys. Lett.*, 2010, 96, 063501.
117. S.-Q. Fan, B. Fang, J. H. Kim, B. Jeong, C. Kim, J.-S. Yu and J. Ko, *Langmuir*, 2010, 26, 13644-13649.
118. M. Seol, E. Ramasamy, J. Lee and K. Yong, *J. Phys. Chem. C*, 2011, 115, 22018-22024.
119. P. Sudhagar, E. Ramasamy, W.-H. Cho, J. Lee and Y. S. Kang, *Electrochem. Commun.*, 2011, 13, 34-37.
120. G. S. Paul, J. H. Kim, M.-S. Kim, K. Do, J. Ko and J.-S. Yu, *ACS Appl. Mater. Interfaces*, 2012, 4, 375-381.
121. J. Dong, S. Jia, J. Chen, B. Li, J. Zheng, J. Zhao, Z. Wang and Z. Zhu, *J. Mater. Chem.*, 2012, 22, 9745-9750.
122. F. Hao, P. Dong, J. Zhang, Y. Zhang, P. E. Loya, R. H. Hauge, J. Li, J. Lou and H. Lin, *Sci. Rep.*, 2012, 2.
123. X. Fang, T. Ma, G. Guan, M. Akiyama, T. Kida and E. Abe, *J. Electroanal. Chem.*, 2004, 570, 257-263.
124. D. Reynolds, G. Leies, L. Antes and R. Marburger, *Phys. Rev.*, 1954, 96, 533.
125. Y. Zhao and C. Burda, *Energy Environ. Sci.*, 2012, 5, 5564-5576.
126. Y. Zhao, H. Pan, Y. Lou, X. Qiu, J. Zhu and C. Burda, *J. Am. Chem. Soc.*, 2009, 131, 4253-4261.
127. Z. Peng, Y. Liu, Y. Zhao, K. Chen, Y. Cheng and W. Chen, *Electrochim. Acta*, 2014, 135, 276-283.
128. G. S. Selopal, I. Concina, R. Milan, M. M. Natile, G. Sberveglieri and A. Vomiero, *Nano Energy*, 2014, 6, 200-210.
129. S. Wang, W. Dong, X. Fang, S. Zhou, J. Shao, Z. Deng, R. Tao, Q. Zhang, L. Hu and J. Zhu, *Electrochim. Acta*, 2015, 154, 47-53.
130. L. Quan, W. Li, L. Zhu, X. Chang and H. Liu, *RSC Adv.*, 2014, 4, 32214-32220.
131. K. Zhao, H. Yu, H. Zhang and X. Zhong, *J. Phys. Chem. C*, 2014, 118, 5683-5690.
132. Y.-F. Xu, W.-Q. Wu, H.-S. Rao, H.-Y. Chen, D.-B. Kuang and C.-Y. Su, *Nano Energy*, 2015, 11, 621-630.
133. C. Shen, L. Sun, Z. Y. Koh and Q. Wang, *J. Mater. Chem. A*, 2014, 2, 2807-2813.
134. H. Salaramoli, E. Maleki, Z. Shariatinia and M. Ranjbar, *J. Photochem. Photobiol. A*, 2013, 271, 56-64.
135. M. Deng, S. Huang, Q. Zhang, D. Li, Y. Luo, Q. Shen, T. Toyoda and Q. Meng, *Chem. Lett.*, 2010, 39, 1168-1170.
136. I. Mora-Seró, S. Giménez, T. Moehl, F. Fabregat-Santiago, T. Lana-Villareal, R. Gómez and J. Bisquert, *Nanotechnology*, 2008, 19, 424007.
137. Y. Jiang, X. Zhang, Q.-Q. Ge, B.-B. Yu, Y.-G. Zou, W.-J. Jiang, W.-G. Song, L.-J. Wan and J.-S. Hu, *Nano Lett.*, 2013, 14, 365-372.
138. Y. Jiang, X. Zhang, Q.-Q. Ge, B.-B. Yu, Y.-G. Zou, W.-J. Jiang, J.-S. Hu, W.-G. Song and L.-J. Wan, *ACS Appl. Mater. Interfaces*, 2014, 6, 15448-15455.
139. M. Ye, C. Chen, N. Zhang, X. Wen, W. Guo and C. Lin, *Adv. Energy Mater.*, 2014, 4.
140. M. Deng, Q. Zhang, S. Huang, D. Li, Y. Luo, Q. Shen, T. Toyoda and Q. Meng, *Nanoscale Res. Lett.*, 2010, 5, 986-990.
141. D.-M. Li, L.-Y. Cheng, Y.-D. Zhang, Q.-X. Zhang, X.-M. Huang, Y.-H. Luo and Q.-B. Meng, *Sol. Energy Mater. Sol. Cells*, 2014, 120, 454-461.
142. F. Wang, H. Dong, J. Pan, J. Li, Q. Li and D. Xu, *J. Phys. Chem. C*, 2014, 118, 19589-19598.
143. A. D. Savariraj, K. Viswanathan and K. Prabakar, *Electrochim. Acta*, 2014, 149, 364-369.
144. L. Li, P. Zhu, S. Peng, M. Srinivasan, Q. Yan, A. S. Nair, B. Liu and S. Samakrishna, *J. Phys. Chem. C*, 2014, 118, 16526-16535.
145. P. Lukashev, W. R. Lambrecht, T. Kotani and M. v. Schilfgaarde, *Phys. Rev. B*, 2007, 76, 195202.
146. C. S. Kim, S. H. Choi and J. H. Bang, *ACS Appl. Mater. Interfaces*, 2014, 6, 22078-22087.
147. J. L. Da Silva, S.-H. Wei, J. Zhou and X. Wu, *Appl. Phys. Lett.*, 2007, 91, 091902.
148. M. Buerger and B. J. Wuensch, *Science*, 1963, 141, 276-277.
149. M. Kundu, T. Hasegawa, K. Terabe and M. Aono, *J. Appl. Phys.*, 2008, 103, 073523.
150. W. Chen, M. Wang, T. Qian, H. Cao, S. Huang, Q. He, N. Liang, C. Wang and J. Zai, *Nano Energy*, 2015, 12, 186-196.
151. M. Ye, X. Wen, N. Zhang, W. Guo, X. Liu and C. Lin, *Journal of Materials Chemistry A*, 2015, 3, 9595-9600.
152. A. D. Savariraj, K. K. Viswanathan and K. Prabakar, *ACS Appl. Mater. Interfaces*, 2014, 6, 19702-19709.
153. H.-J. Kim, J.-H. Kim, C. S. P. Kumar, D. Punnoose, S.-K. Kim, C. V. Gopi and S. S. Rao, *J. Electroanal. Chem.*, 2015, 739, 20-27.
154. C. V. Gopi, M. Venkata-Haritha, S.-K. Kim, S. S. Rao, D. Punnoose and H.-J. Kim, *RSC Adv.*, 2015, 5, 2963-2967.
155. Y. Zhang, J. Tian, H. Li, L. Wang, X. Qin, A. M. Asiri, A. O. Al-Youbi and X. Sun, *Langmuir*, 2012, 28, 12893-12900.
156. H. Chen, L. Zhu, H. Liu and W. Li, *J. Phys. Chem. C*, 2013, 117, 3739-3746.
157. W. L. Chen, M. Wang, T. Y. Qian, H. L. Cao, S. S. Huang, Q. Q. He, N. Liang, C. Wang and J. T. Zai, *Nano Energy*, 2015, 12, 186-196.
158. M. Ye, X. Wen, N. Zhang, W. Guo, X. Liu and C. Lin, *J. Mater. Chem. A*, 2015, 3, 9595-9600.

159. Z. Yang, C.-Y. Chen and H.-T. Chang, *Sol. Energy Mater. Sol. Cells*, 2011, 95, 2867-2873.
160. W. Guo, C. Chen, M. Ye, M. Lv and C. Lin, *Nanoscale*, 2014, 6, 3656-3663.
161. M. Que, W. Guo, X. Zhang, X. Li, Q. Hua, L. Dong and C. Pan, *J. Mater. Chem. A*, 2014, 2, 13661-13666.
162. W. Guo, X. Zhang, R. Yu, M. Que, Z. Zhang, Z. Wang, Q. Hua, C. Wang, Z. L. Wang and C. Pan, *Adv. Energy Mater.*, 2015, 5, 1500141.
163. Z. Tachan, M. Shalom, I. Hod, S. Rühle, S. Tirosh and A. Zaban, *J. Phys. Chem. C*, 2011, 115, 6162-6166.
164. Z. Yang, C.-Y. Chen, C.-W. Liu and H.-T. Chang, *Chem. Commun.*, 2010, 46, 5485-5487.
165. H. Geng, L. Zhu, W. Li, H. Liu, L. Quan, F. Xi and X. Su, *J. Power Sources*, 2015, 281, 204-210.
166. H. J. Kim, T. B. Yeo, S. K. Kim, S. S. Rao, A. D. Savariraj, K. Prabakar and C. V. Gopi, *Eur. J. Inorg. Chem.*, 2014, 2014, 4281-4286.
167. A. D. Mani, M. Deepa, P. Ghosal and C. Subrahmanyam, *Electrochim. Acta*, 2014, 139, 365-373.
168. H.-J. Kim, D.-J. Kim, S. S. Rao, A. D. Savariraj, K. Soo-Kyoung, M.-K. Son, C. V. Gopi and K. Prabakar, *Electrochim. Acta*, 2014, 127, 427-432.
169. Z. Yang, C. Y. Chen, C. W. Liu, C. L. Li and H. T. Chang, *Adv. Energy Mater.*, 2011, 1, 259-264.
170. H. Yuan, J. Lu, X. Xu, D. Huang, W. Chen, Y. Shen and M. Wang, *J. Electrochem. Soc.*, 2013, 160, H624-H629.
171. Y. Yang, L. Zhu, H. Sun, X. Huang, Y. Luo, D. Li and Q. Meng, *ACS Appl. Mater. Interfaces*, 2012, 4, 6162-6168.
172. P. Parand, M. Samadpour, A. Esfandiar and A. Iraji Zad, *ACS Photonics*, 2014, 1, 323-330.
173. M. Eskandari, V. Ahmadi and R. Ghahary, *Electrochim. Acta*, 2015, 151, 393-398.
174. X. Song, M. Wang, J. Deng, Y. Ju, T. Xing, J. Ding, Z. Yang and J. Shao, *J. Power Sources*, 2014, 269, 661-670.
175. M. S. Faber, M. A. Lukowski, Q. Ding, N. S. Kaiser and S. Jin, *J. Phys. Chem. C*, 2014, 118, 21347-21356.
176. X. Zhang, X. Huang, Y. Yang, S. Wang, Y. Gong, Y. Luo, D. Li and Q. Meng, *ACS Appl. Mater. Interfaces*, 2013, 5, 5954-5960.
177. J. Xu, X. Yang, Q.-D. Yang, T.-L. Wong and C.-S. Lee, *J. Phys. Chem. C*, 2012, 116, 19718-19723.
178. Y. Cao, Y. Xiao, J.-Y. Jung, H.-D. Um, S.-W. Jee, H. M. Choi, J. H. Bang and J.-H. Lee, *ACS Appl. Mater. Interfaces*, 2013, 5, 479-484.
179. Y. Zhang, C. Shi, X. Dai, F. Liu, X. Fang and J. Zhu, *Electrochim. Acta*, 2014, 118, 41-44.
180. X. Zeng, W. Zhang, Y. Xie, D. Xiong, W. Chen, X. Xu, M. Wang and Y.-B. Cheng, *J. Power Sources*, 2013, 226, 359-362.
181. J. Xiao, X. Zeng, W. Chen, F. Xiao and S. Wang, *Chem. Commun.*, 2013, 49, 11734-11736.
182. H. Ahari, C. L. Bowes, T. Jiang, A. Lough, G. A. Ozin, R. L. Bedard, S. Petrov and D. Young, *Adv. Mater.*, 1995, 7, 375-378.
183. W. Wang, Y. Geng, P. Yan, F. Liu, Y. Xie and Y. Qian, *J. Am. Chem. Soc.*, 1999, 121, 4062-4063.
184. V. Colvin, M. Schlamp and A. Alivisatos, *Nature*, 1994, 370, 354-357.
185. F. Gong, H. Wang, X. Xu, G. Zhou and Z.-S. Wang, *J. Am. Chem. Soc.*, 2012, 134, 10953-10958.
186. H. M. Choi, I. A. Ji and J. H. Bang, *ACS Appl. Mater. Interfaces*, 2014, 6, 2335-2343.
187. F. Bo, C. Zhang, C. Wang, S. Xu, Z. Wang and Y. Cui, *J. Mater. Chem. A*, 2014, 2, 14585-14592.
188. F. Liu, J. Zhu, L. Hu, B. Zhang, J. Yao, M. K. Nazeeruddin, M. Gratzel and S. Dai, *J. Mater. Chem. A*, 2015, 3, 6315-6323.
189. X. Q. Chen, Z. Li, Y. Bai, Q. Sun, L. Z. Wang and S. X. Dou, *Chem. Eur. J.*, 2015, 21, 1055-1063.
190. C. Ma, Q. Tang, D. Liu, Z. Zhao, B. He, H. Chen and L. Yu, *J. Power Sources*, 2015, 276, 215-221.
191. C. Ma, Q. Tang, Z. Zhao, M. Hou, Y. Chen, B. He and L. Yu, *J. Power Sources*, 2015, 278, 183-189.
192. J. Xu, X. Yang, Q. Yang, W. Zhang and C.-S. Lee, *ACS Appl. Mater. Interfaces*, 2014, 6, 16352-16359.

This article reviews the application of metal chalcogenide counter electrodes in quantum dot sensitized solar cells.